ACS OMEGA

http://pubs.acs.org/journal/acsodf

Article

Oxidative MLD of Conductive PEDOT Thin Films with EDOT and $ReCl_5$ as Precursors

Saba Ghafourisaleh, Georgi Popov, Markku Leskelä, Matti Putkonen, and Mikko Ritala*

Cite This: *ACS Omega* 2021, 6, 17545−17554

Read Online

ACCESS | Metrics & More | Article Recommendations

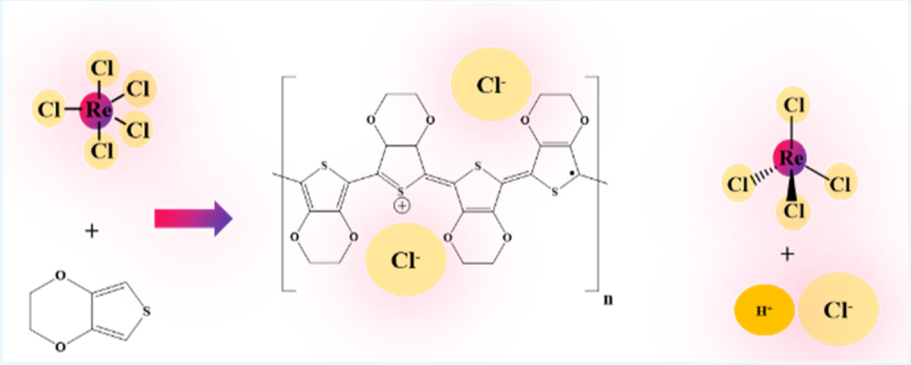

ABSTRACT: Because of its high conductivity and intrinsic stability, poly(3,4-ethylenedioxythiophene (PEDOT) has gained great attention both in academic research and industry over the years. In this study, we used the oxidative molecular layer deposition (oMLD) technique to deposit PEDOT from 3,4-ethylenedioxythiophene (EDOT) and a new inorganic oxidizing agent, rhenium pentachloride ($ReCl_5$). We extensively characterized the properties of the films by scanning electron microscopy, X-ray diffraction, X-ray photoelectron spectroscopy (XPS), energy-dispersive X-ray spectroscopy (EDS), Raman, and conductivity measurements. The oMLD of polymers is based on the sequential adsorption of the monomer and its oxidation-induced polymerization. However, oMLD has been scarcely used because of the challenge of finding a suitable combination of volatile, reactive, and stable organic monomers applicable at high temperatures. $ReCl_5$ showed promising properties in oMLD because it has high thermal stability and high oxidizing ability for EDOT. PEDOT films were deposited at temperatures of 125−200 °C. EDS and XPS measurements showed that the as-deposited films contained residues of rhenium and chlorine, which could be removed by rinsing the films with deionized water. The polymer films were transparent in the visible region and showed relatively high electrical conductivities within the 2−2000 S cm^{-1} range.

1. INTRODUCTION

Poly(3,4-ethylenedioxythiophene) (PEDOT) is one of the best-known conjugated conductive polymers that has been extensively studied for decades.[1] Other well-known conjugated conductive polymers, polypyrrole and polyacetylene, were discovered earlier in the pioneering work of Shirakawa et al.[2−4]

Compared to the other conductive polymers, PEDOT has attracted lots of attention because of its high and stable electrical conductivity. Electrical conductivities up to 8797 S cm^{-1} and 7520 S cm^{-1} have been reported for single crystals[5] and thin films,[6] respectively. These conductivity values are just 1 order of magnitude lower than those of the most conductive metals such as silver and copper.[7] Conductive polymers are often highlighted for their mechanical, electrical, optoelectronic, thermoelectric, photovoltaic, and lighting properties both academically and industrially. The significant importance of PEDOT is acknowledged through the high number of applications in thermoelectricity, photovoltaics, lighting, sensing, technical coatings, transparent electrodes, bioelectronics, and so forth.[8−14]

Although there are a myriad of publications dealing with the synthesis, properties, conductivity enhancement, and different applications of PEDOT, there is still room for a deeper understanding of the materials' properties, whereas novel deposition methods can enable its use in new applications. PEDOT thin films can be deposited by both liquid- and gas-phase methods. In situ chemical polymerization (ICP)[15−19] was the first and widely utilized film-forming method that

Received: April 16, 2021
Accepted: June 23, 2021
Published: July 1, 2021

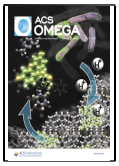

electrochemically synthesizes PEDOT. Oxidative ICP was carried out in EDOT solutions with chemical oxidants such as metal salts, peroxides, and other more sophisticated oxidants.[8] Typically, ICP of PEDOT results in high conductivity, poor transparency, and small sample sizes.[20] Another promising approach is based on spin-casting of the 3,4-ethylenedioxythiophene (EDOT) monomer and oxidizing agents onto a variety of different substrates to oxidatively polymerize the monomers. Films with high transparency and conductivity values of 300 S cm^{-1} have been reported.[21] PEDOT and other conductive polymer films have also been electrodeposited for different applications.[22,23] For instance, electrodeposition of polyaniline (PANI)-PEDOT on an indium tin oxide substrate with gold nanostructures was reported by Popov et al.[24] as an example of enhancing the electrochromic properties of conductive polymers. Moreover, a comparison study on the electrical conductivity of the electrodeposited polymer films such as PEDOT, PANI, and nanocomposite of PANI-PEDOT has been reported.[25]

Vapor-phase polymerization (VPP)[20,26−28] is based on a similar concept to ICP, but instead of mixing EDOT to the oxidant solution, oxidants adsorbed on a substrate surface are exposed to EDOT vapors.[20] A recent approach to the PEDOT film deposition is chemical vapor deposition (CVD)[29−34] using EDOT and $FeCl_3$,[5,35] Br_2,[36] $MoCl_5$,[37] $SbCl_5$,[38] or $VOCl_3$[39] as an oxidant. Both gas-phase techniques, VPP and CVD, rely on the oxidation of the EDOT monomer by an oxidant, and a similar approach has been used also with oxidative molecular layer deposition (oMLD).[37] The principle of MLD[40−42] is stemming from the atomic layer deposition (ALD) technique.[43,44] In both methods, film growth occurs through self-limiting surface reactions between alternately supplied precursor vapors. The self-limiting film growth mechanism gives ALD and MLD superior characteristics as compared to the competing methods: uniform and conformal films over also large and three-dimensionally structured substrates, and accurate and simple film thickness control. Previously, Atanasov et al.[37] used $MoCl_5$ as an oxidant together with the EDOT monomer for the oMLD of PEDOT thin films. The films were deposited at temperatures of 100−150 °C. According to X-ray photoelectron spectroscopy (XPS) analysis, approximately 6 at. % residuals from $MoCl_5$ with different oxidation states of Mo were present in the films exposed to ambient air after the deposition. In an attempt to improve the film purity, we studied PEDOT thin film deposition by the oMLD technique using alternative oxidizers. Inspired by the $MoCl_5$-based process, we explored oxidizers, which have been previously used for oxidation of thiophene monomer derivatives in CVD such as Br_2, $SbCl_5$, and $VOCl_3$.[36,38,39] Rhenium pentachloride ($ReCl_5$) was identified as another potential oxidizer based on its similar properties and structure to $MoCl_5$. To the best of our knowledge, there are no previous reports on using $ReCl_5$ as an oxidizer.

2. RESULTS AND DISCUSSION

2.1. PEDOT Film Growth. In the initial experiments besides $ReCl_5$, bromine, antimony pentachloride, vanadium oxytrichloride, and ozone were used as oxidizers, but only $ReCl_5$ led to PEDOT deposition.

Atanasov et al.[37] demonstrated the deposition of PEDOT thin films in the 100−150 °C temperature range with $MoCl_5$. $ReCl_5$ is structurally and chemically similar to $MoCl_5$, with a similar oxidation potential for the EDOT oxidation. In our present study, somewhat higher deposition temperatures were needed because the source temperature of $ReCl_5$ was 110−115 °C. We were able to deposit PEDOT thin films in the temperature range of 125−200 °C. Films deposited at 200 °C were uniform, reflective on silicon, and transparent on soda-lime glass (Figure 1). Increasing the temperature to above 200

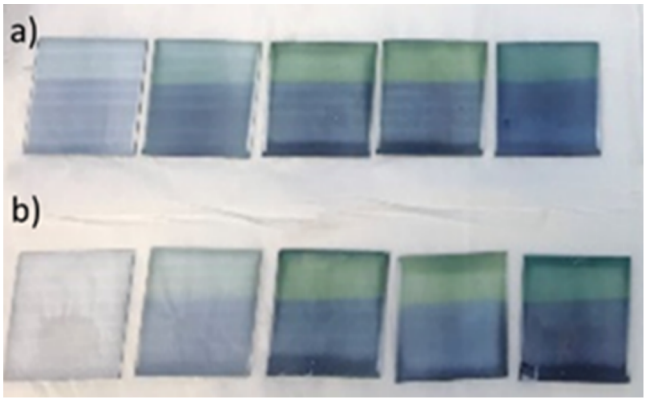

Figure 1. Photograph of the films deposited at 200 °C with 1000 cycles on soda-lime glass substrates and dipped halfway in water (lower half), using (0.2, 0.5, 1.0, 2.5, and 3.0 s) pulses. (a) $ReCl_5$ and (b) EDOT.

°C decreased the growth rate dramatically and no film was achieved at temperatures higher than 200 °C. Deposition temperatures lower than 200 °C had a considerable effect on the film quality and appearance. Films deposited at these temperatures were flaky, nonuniform, and opaque black. Therefore, 200 °C was selected as a temperature to deposit PEDOT films for further analysis.

The effect of precursor pulsing times on the deposition process was studied at 200 °C. With both precursors, no full saturation of the growth rate was observed (Figure 2). This was unexpected because EDOT and $ReCl_5$ are reported to be stable at the temperatures in question.[45]

The PEDOT polymer is assumed to be deposited through a self-limiting radical cation (RC) transition mechanism.[46−48] During the $ReCl_5$ pulse, a monolayer of $ReCl_5$ is chemisorbed on the surface. During the EDOT pulse, $ReCl_5$ oxidizes EDOT and transforms it into a RC (Scheme 1a) that dimerizes (Scheme 1b) and is rapidly stabilized through removal of the two protons by chloride anions as counter ions and dopants (Scheme 1c). Additional $ReCl_5$ oxidizes the dimers and the chain growth continues as a classical step-polymerization forming the PEDOT polymer (Scheme 1d). Once all $ReCl_5$ is consumed from the surface, the growth stops. The next $ReCl_5$ pulse adds a new layer of $ReCl_5$ molecules on the surface to continue the growth. $ReCl_5$ also oxidizes the PEDOT chains into a doped (conducting) state. Some of the chloride anions released through this process can get trapped in the polymer media and act as counter ions for the polymer cations to stabilize the polymer structure. These interactions can also enhance the electrical conductivity properties of the polymer. Polymer is self-doped after the polymerization and can efficiently conduct electricity as will be seen later.

As the polymerization continues, the oligomeric PEDOT chains can appear in three molecular structures; neutral, RC, and dication (DC) (Figure 2). Because PEDOT is a conjugated conductive polymer, the charge carriers created

https://doi.org/10.1021/acsomega.1c02029
ACS Omega 2021, 6, 17545−17554

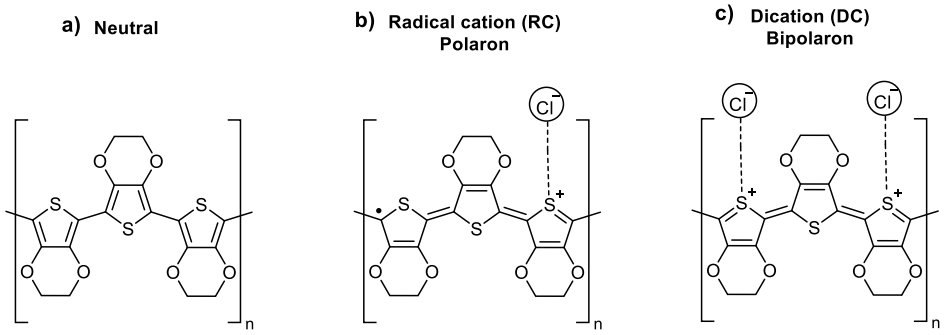

Figure 2. PEDOT oligomer chains with three molecular structures. (a) Neutral, (b) RC or polaron, and (c) DC or bipolaron structure.

Scheme 1. Possible Mechanism for the Polymerization of the EDOT by $ReCl_5$. (a) Dimerization, (b) stabilization by Chloride Anions, (c) removal of the Protons, and (d) Polymerization

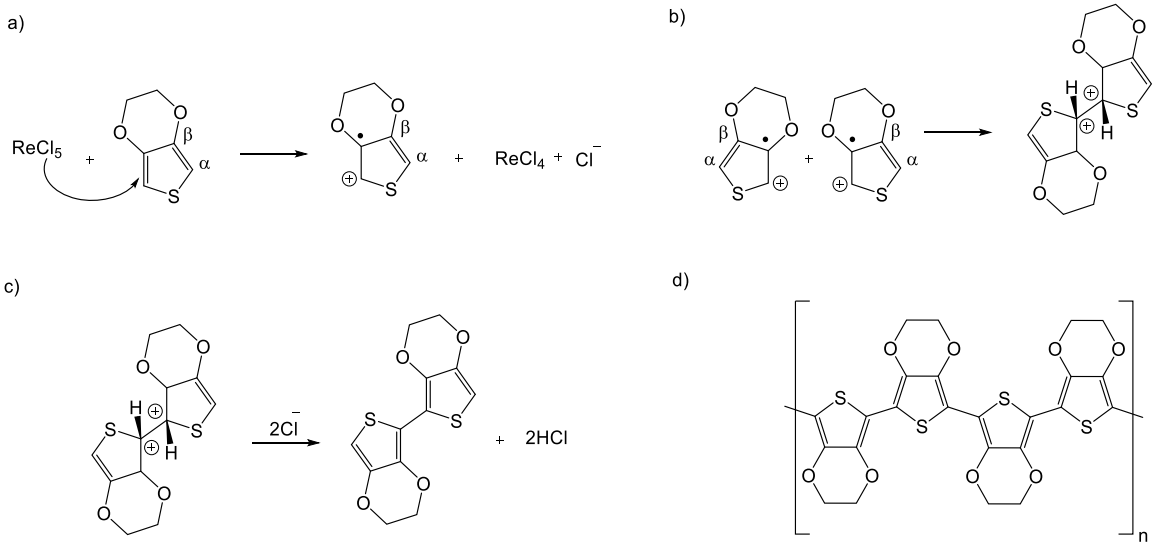

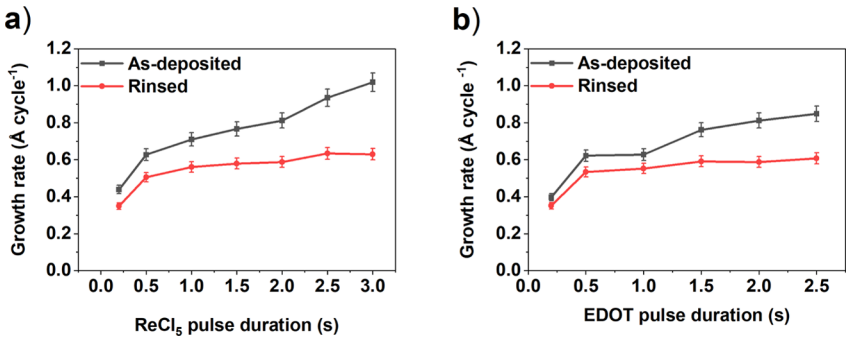

Figure 3. Growth rates of the films deposited at 200 °C by varying the pulsing durations of (a) $ReCl_5$ and (b) EDOT.

by doping with chloride ions are in nondegenerate energy levels consisting of polarons (RC) and bipolarons (DC).

As discussed in more detail later, according to energy-dispersive X-ray spectroscopy (EDS), the film surfaces had Re- and chlorine-containing particulates originating from $ReCl_5$. As PEDOT is insoluble in water, rinsing with water was tested and indeed the particulates could be easily removed by rinsing the films with deionized water at 25 °C.

On glass, the films were clearly transparent. The as-deposited films were gray-green due to the residual impurities. The films became blue and maintained their transparency and uniformity after the rinsing (Figure 1). PEDOT in its natural doped state has a sky-blue color. There are various factors that can change the color of the polymer.[9]

The water rinsing after the deposition caused a 20% thickness decrease (from 63−71 to 51−56 nm) for the films deposited with the shortest pulsing times of 0.5−1.0 s, whereas the films deposited with a 2.0 s $ReCl_5$ pulse time encountered a 27% thickness decrease (from 81 to 59 nm). Once the growth rates were evaluated from the rinsed thin films, they showed better saturation and remained relatively constant around 0.5 Å $cycle^{-1}$ when the $ReCl_5$ or EDOT pulse times were increased (Figure 3).

2.2. Electrical and Optical Properties. We studied the electrical conductivity of our films by measuring the sheet

https://doi.org/10.1021/acsomega.1c02029
ACS Omega 2021, 6, 17545−17554

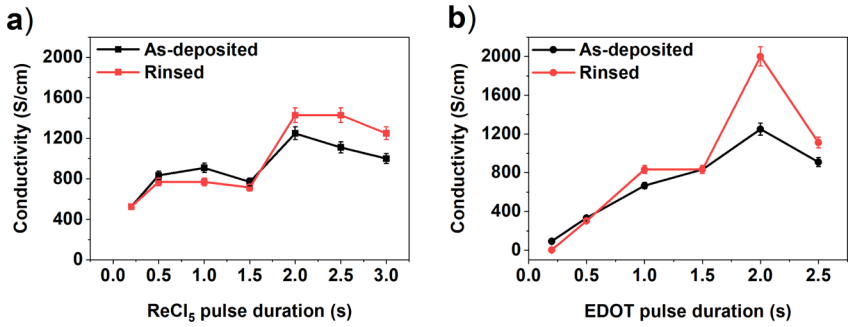

Figure 4. Conductivity of the as-deposited and water-rinsed samples. Effect of (a) $ReCl_5$ pulse duration and (b) EDOT pulse duration.

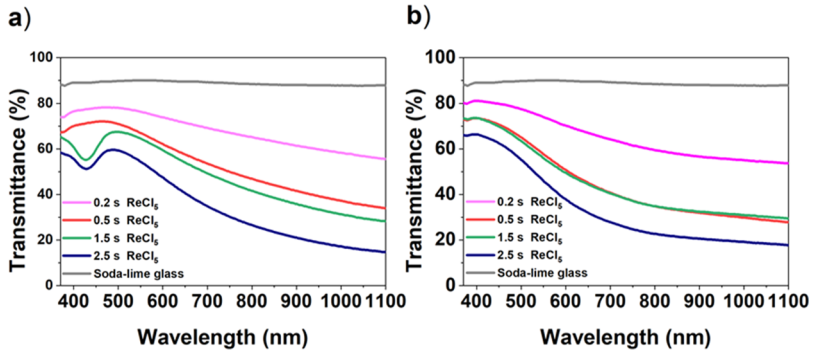

Figure 5. Transmittance of the (a) as-deposited films with various $ReCl_5$ pulse lengths and (b) transmittance of the rinsed films.

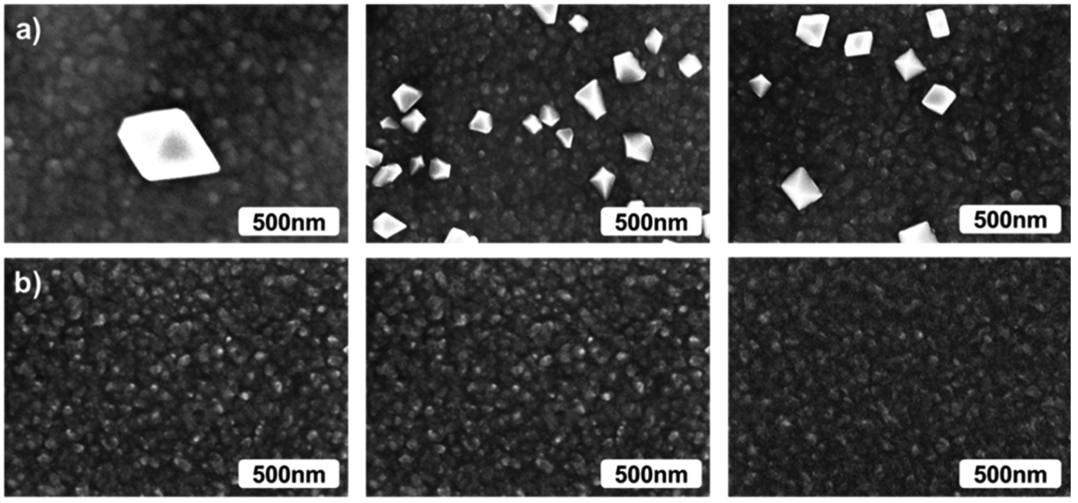

Figure 6. SEM images of (a) as-deposited and (b) water-rinsed PEDOT films deposited with 1000 cycles at 200 °C using, from left to right, 0.2, 0.5, and 1.0 s pulses of $ReCl_5$.

resistance with a four-point probe. In order to compare the electrical conductivity of the films before and after the postdeposition water-rinse, we dipped the films on glass substrates only halfway to water (Figure 1) and the thicknesses and electrical conductivities of the two-halves were measured and compared (Figure 4).

We measured conductivities exceeding 2000 S cm^{-1}. The conductivities of the thicker films increased after the water rinsing, whereas in the thinner films the water rinsing did not cause any significant conductivity changes.

PEDOT films deposited with various deposition methods[53−57] have had different conductivities. There have been numerous studies on enhancement of the conductivities of PEDOT thin films, where the conductivity was enhanced by dopant treatments after the deposition.[7,19,33,37,46,50] For instance, Song et al.[53] reported a conductivity of 2673 S cm^{-1} for flexible high-conductivity transparent electrode based on PEDOT: poly(styrene sulfonate) (PEDOT:PSS) deposited on flexible plastic substrates via a H_2SO_4 treatment. This was among the highest electrical conductivities of PEDOT:PSS films processed on flexible substrates. The electrodes demonstrated high transparency, over 60%, at 550 nm.

Heydari Gharahcheshmeh et al.[6] reported an optimized electrical conductivity of 7520 ± 240 S cm^{-1}, which is a record for PEDOT thin films. These films were face-on oriented semicrystalline PEDOT and were deposited by water-assisted oxidative chemical vapor deposition with antimony pentachloride as an oxidant. To the best of our knowledge, 8797 S

https://doi.org/10.1021/acsomega.1c02029
ACS Omega 2021, 6, 17545−17554

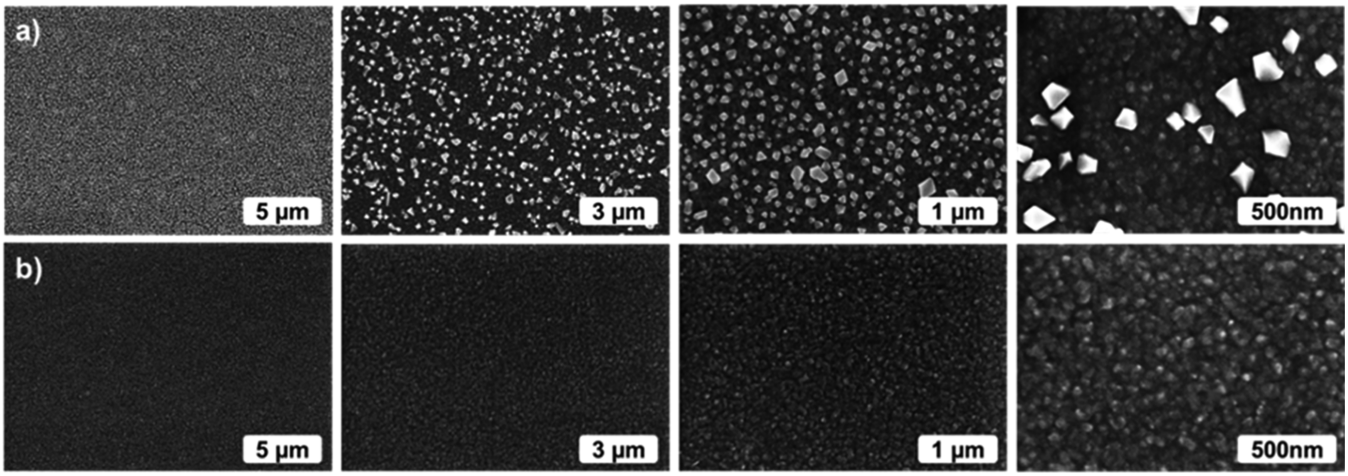

Figure 7. SEM images at different magnifications of (a) as-deposited and (b) water-rinsed PEDOT films deposited with 1000 cycles at 200 °C using, a 0.5 s pulse of $ReCl_5$.

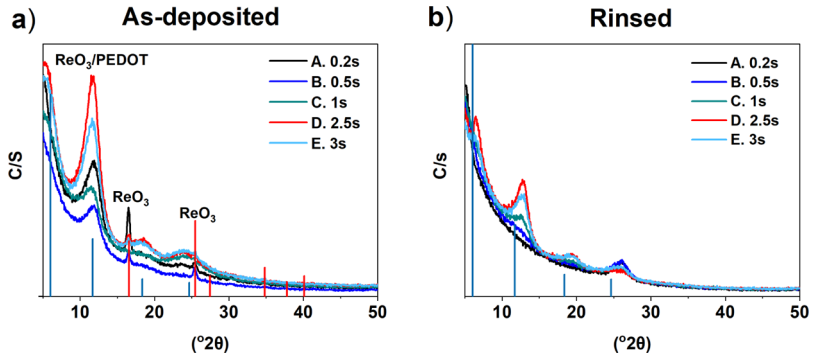

Figure 8. GIXRD reflection patterns of PEDOT films on Si. Films were deposited at 200 °C with 1000 cycles. (a) $ReCl_5$ pulse, EDOT pulse, and purge durations were (0.2, 0.5, 1, 2.5, and 3 s), 2.0 s, and 2.0 s, respectively. (b) After the water rinsing. The bars indicate positions of reflections measured from the spin-casted PEDOT films (blue bars)[58] and ReO_3 (red bars).[59]

cm^{-1} is the highest conductivity that has been measured for PEDOT single crystals.[5]

Generally, conductivity is highly affected by the orientation of semicrystalline-conjugated polymers, which is strongly influenced by the fabrication method, size of the counter-ion dopant, and process parameters.[49] The predominant edge-on orientation is frequently reported in PEDOT:PSS, PEDOT:Tos, and PEDOT:OTf processes,[19,51,52] while the use of smaller counter-ion dopants such as chloride (Cl^-) induces the predominant face-on orientation in PEDOT:Cl thin films.[39,50]

Most of the conductivities reported for PEDOT thin films in their natural self-doped state have been around 1000 S cm^{-1}.[7] Compared to these values, the films deposited by our process without any extra doping treatments showed somewhat higher electrical conductivities.

To confirm the effect of the water rinsing on the transparency of the PEDOT films, their transmittance was measured with a UV/Vis spectrometer with a bare soda-lime glass as the reference (Figure 5). The rinsed films showed higher transmittance than the as-deposited films. For the rinsed films, the highest transmittance value was 80%, while the corresponding value for the as-deposited film was 75%.

With increasing thickness of the films, the transparency decreased. In the thicker as-deposited films, there is one dip in transmittance at 425 nm for 1.5 and 2.5 s pulses of $ReCl_5$, but this dip disappeared after the water rinsing.

2.3. Film Structure and Composition. Scanning electron microscopy (SEM) images showed that the as-deposited films are continuous, but segregated particulates were present on their surface (Figure 6a). EDS analysis indicated that the particulates contained rhenium and chlorine impurities. Effects of the $ReCl_5$ pulse times on the film morphology can be seen in SEM images (Figure 6a). It appears that the amount of particulates increases with the increasing $ReCl_5$ pulse time, thus at least partially explaining the nonsaturating growth observed in the as-deposited films while increasing precursor pulse times (Figure 3). After the water rinsing, the particulates had been removed from the film surfaces (Figure 6b). Some Re impurities were still measured with EDS but no chlorine could be detected.

In order to show the coverage of the particulates on the film surface after the deposition in detail, we imaged the surface morphologies of the PEDOT film deposited with 0.5 s pulses of $ReCl_5$ in different magnifications (Figure 7a). After the water rinsing, the particulates were again removed from the film surface (Figure 7b).

GIXRD studies on the PEDOT thin films were performed in order to identify the PEDOT structure as well as to identify the rhenium- and chlorine-containing particulates left on the film surface after the deposition. We compared our X-ray diffraction (XRD) results to those reported by Aasmundtveit et al.[58] who studied PEDOT crystallinity with synchrotron radiation. It has been reported earlier[7] that PEDOT has a paracrystalline

https://doi.org/10.1021/acsomega.1c02029
ACS Omega 2021, 6, 17545−17554

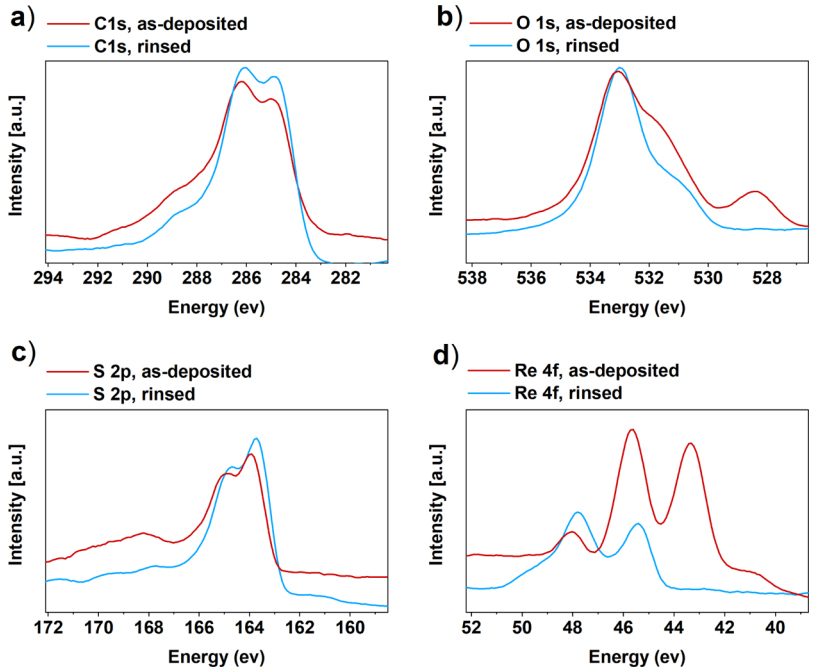

Figure 9. XPS results measured from the as-deposited and water-rinsed films. (a) Carbon 1s, (b) oxygen 1s, (c) rhenium 4f, and (d) sulfur 2p.

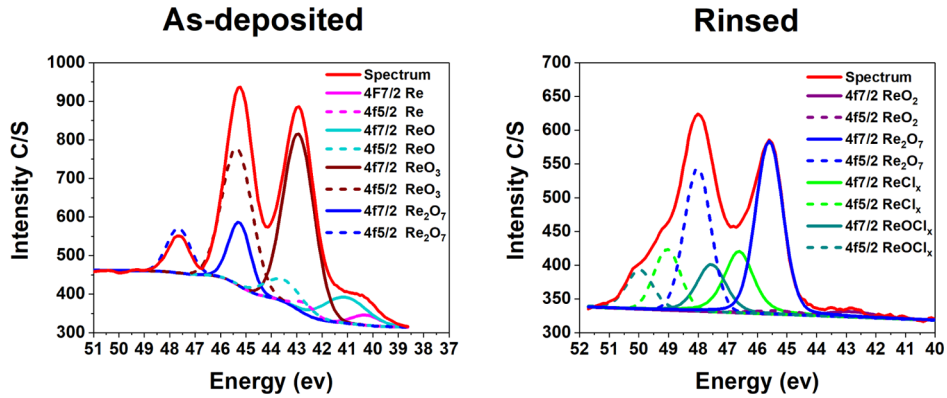

Figure 10. Re 4f curve fit for four oxidation states for the as-deposited and water-rinsed films.

structure with broad X-ray reflections without long-range order. This was seen also in all the diffraction patterns of our films, as broad reflections were observed that match with the PEDOT structure (Figure 8).

The as-deposited PEDOT films deposited with short $ReCl_5$ precursor pulses of 0.2, 0.5, and 1.0 s additionally had reflections that matched with the ReO_3 structure (Figure 7a). These reflections disappeared upon rinsing with water, which implies that ReO_3 was in the particles that were removed by the rinsing (Figure 8b).

Detailed compositional studies with XPS confirmed the presence of carbon, sulfur, and oxygen. Chlorine was not detected in the as-deposited or water-rinsed PEDOT films but rhenium impurities in different oxidation states were detected. In the as-deposited films, there were 1.6 at. % Re and in the water-rinsed 0.5 at. %. These residual concentrations compare favorably with the 6 at. % Mo found from the PEDOT films deposited using $MoCl_5$ as the oxidant.[37] Figure 9 represents the spectra of each element. The carbon 1s peak is a singlet and the expected peaks for PEDOT are at 285.0 and 286.1 eV positions in a 1:2 ratio,[16,60] but instead the peak at 284.7−285 eV was more intense because of hydrocarbon contamination. Contaminants are probably the reason for the tails at 287−289 eV, which refer to carbonyl groups.

The main oxygen 1s peak at 533.6 eV is from PEDOT,[16,61] and the shoulder at 531 eV is probably due to contamination (hydroxides). A special feature found in the as-deposited film is the peak at 528.3 eV that could be from rhenium oxide; that peak was absent in the spectrum of the water-rinsed sample. Sulfur 2p-doublet peaks at 163.5 eV ($2p_{3/2}$) and 164.7 eV ($2p_{1/2}$) are from PEDOT.[16,60]

Water rinsing decreased the Re content from 1.6 to 0.5 at. %. Although the large ReO_3-containing particulates were removed by rinsing, some Re was still left in the films. Rhenium 4f-line is a doublet and it seems to consist of four different oxidation states (0, II, VI, and VII) for the as-deposited film, whereas for the water-rinsed film besides the IV and VII oxidation states, $ReCl_x$ and $ReOCl_x$ were identified. While no chlorine itself could be detected with XPS, the films could still contain such minor amounts of chlorine that affected the Re peak positions. Therefore, it was not trivial to fit the data to identify the oxidation state of rhenium in the chloride, oxide, and

https://doi.org/10.1021/acsomega.1c02029
ACS Omega 2021, 6, 17545−17554

oxychloride compounds. Therefore, the curve fit was made for four components.[62]

From the relative intensities, one can calculate that rhenium detected in the as-deposited film (1.6 at. % in total) consisted of the following oxidation states: 3% metallic Re, 13% Re(II), 66% Re(VI), and 17% Re(VII). After the water rinsing, the distribution (0.5 at. % in total) was changed to 3% Re(IV), 57% Re(VII), 24% $ReCl_x$, and 17% $ReOCl_x$ (Figure 10). This further supports that the particulates on the as-deposited films consisted of ReO_3. GIXRD showed reflections that were complying with rhenium in the VI oxidation state. No XRD reflections that would match with the metallic rhenium or rhenium(IV) compounds in the water-rinsed films were observed. The results indicate either the amorphous nature of the rhenium compounds in the zero and IV oxidation states or that the rhenium impurities are dissolved in the PEDOT.

Raman scattering spectroscopy is also a very powerful tool for analyzing and chemical monitoring of PEDOT fingerprints.[63−65] Figure 11 represents the Raman spectra of the PEDOT films deposited with 1.0 and 2.0 s pulse times of $ReCl_5$ and EDOT precursors, respectively.

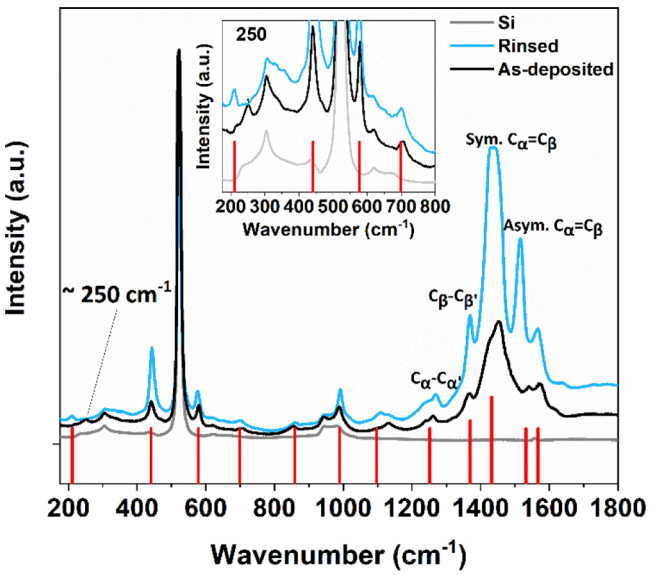

Figure 11. Raman spectra of the PEDOT thin films under green light excitation (λ = 532 nm). The red bars indicate the positions of Raman peaks of the PEDOT structure.

The Raman spectra confirmed the PEDOT structure. The vibrational modes of PEDOT are located at 1532, 1432, 1370, and 1252 cm^{-1}, and assigned to the $C_\alpha{=}C_\beta$ asymmetrical, $C_\alpha{=}C_\beta$ symmetrical, $C_\beta{-}C_{\beta'}$ stretching, and $C_\alpha{-}C_{\alpha'}$ inter-ring stretching vibrations, respectively (see Scheme 2a for the carbon labelling).

PEDOT has two postulated resonance structures in its doped state, quinoid and benzoid forms as depicted in Scheme 2c,d.[66] PEDOT in the benzoid form preserves its aromaticity through the $C_\alpha{-}C_\beta$ bond via two conjugated π-electrons, whereas in the quinoid form there are no conjugated π-electrons on the $C_\alpha{-}C_\beta$ bond and it has more planar structure compared to the benzoid form. The quinoid structure has more rigidity than the benzoid structure. The rigid quinoid structure enables strong interactions between the PEDOT chains and thereby high charge carrier mobility.[33] Raman vibrations indicated the existence of both the rigid quinoid (linear conformation) and benzoid structure (coil conformation) in the doped state of PEDOT.[65]

EDOT monomer as a PEDOT building block also has a considerable effect on the rigid backbone structure of the polymer. The EDOT monomer has two oxygens in its structure and the oxygens play an important role in stabilizing the positive charges and radicals in the conjugated polymer chains.

According to the Raman spectra, PEDOT has an intermediate structure consisting of the $C_\alpha{=}C_\beta$, ($C_\beta{-}C_\beta$, $C_\alpha{-}C_\alpha$) vibrational modes, which are attributed both to the benzoid and quinoid forms in the conjugated backbone of the polymer. There was also a weak mode at ca. 250 cm^{-1} in the as-deposited film that was not seen in the rinsed film. This weak vibrational peak is close to those of ReO_2 (245 cm^{-1})[67] and ReO_3 (243 cm^{-1}).[68]

3. CONCLUSIONS

The oMLD technique is a feasible way to deposit PEDOT thin films. PEDOT thin film deposition was carried out from EDOT and $ReCl_5$. The films with the best qualities were obtained at a deposition temperature of 200 °C, where a growth rate of 0.6 Å $cycle^{-1}$ was measured after water rinsing. After the deposition, there were rhenium and chlorine impurities in the film, but with a postdeposition water rinse, the majority of these impurities were removed. No chlorine was detected by EDS after the water rinse but there were some Re residuals detected by EDS and XPS for the both the as-deposited and water-rinsed films. The films were uniform, transparent, and showed a high electrical conductivity of 2000 S cm^{-1}.

4. MATERIALS AND METHODS

4.1. Film Deposition. The PEDOT thin film depositions were carried out in a hot-wall, flow type F120 ALD reactor

Scheme 2. (a) EDOT, (b) PEDOT, (c) quinoid, and (d) benzoid structures in PEDOT

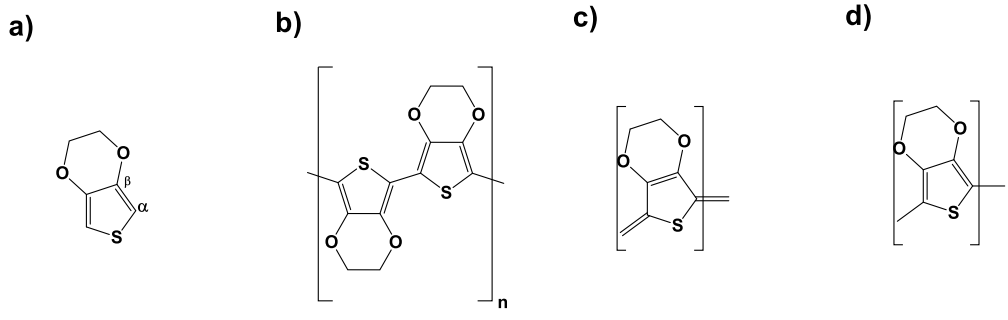

https://doi.org/10.1021/acsomega.1c02029
ACS Omega 2021, 6, 17545−17554

(ASM Microchemistry Ltd.). The pressure inside the reactor was ca. 2 mbar. Monomeric EDOT (TCI, 95−98%) and the oxidants $ReCl_5$ (Strem chemicals, IMC, 99.9%−Re), Br_2 (ACROS organics, >90%, extra pure), $SbCl_5$ (abcr chemicals, 99%), and $VOCl_3$ (abcr chemicals, ≥99%) were used as received. Br_2 and $VOCl_3$ were introduced to the reactor from external containers because of their high volatility at room temperature. $SbCl_5$ is also a highly volatile liquid and was evaporated from an open glass boat inside the reactor at 25−30 °C. EDOT was evaporated and $ReCl_5$ was sublimed from open glass boats inside the reactor at temperatures of 35−45 and 110−115 °C, respectively. Nitrogen (N_2, AGA, 99.999%) was used as a carrier and purging gas. The films were deposited on silicon pieces (5 × 5 cm^2, native oxide) and soda-lime glass substrates. The as-deposited films were rinsed with deionized water at 25 °C.

4.2. Film Characterization. The morphology of the films was studied with a Hitachi S-4800 field emission scanning electron microscope. EDS measurements were performed with an Oxford INCA 350 energy spectrometer connected to the field emission scanning electron microscope. The crystallinity of PEDOT was studied with a Rigaku Smartlab X-ray diffractometer utilizing Cu Kα-radiation in the grazing incidence geometry (GIXRD, incident angle 1°).

Further compositional studies were performed with XPS (Phi Quantum2000) using monochromatized Al Kα-X-rays. The used spot size was 100 μm and the analyzer pass energy was 117.4 eV for the survey and depth profiles and 23.5 eV for the individual peaks.

A confocal Raman microscope (NT-MDT Ntegra) with a 532 nm laser and a 100× objective lens was used to measure the micro-Raman spectra in the backscattering geometry. The nominal output power of the laser was 20 mW. Laser exposure times were 15 s and the number of exposures was 40 for a single measurement.

Resistances of PEDOT thin films deposited on glass substrates were measured at room temperature using a four-point probe instrument (CPS Probe Station, Cascade Microtech combined with Keithley 2400). The as-deposited samples were stored in a desiccator prior to the measurement in order to minimize their exposure to the ambient air.

Film thicknesses were measured using a FS-1 ellipsometer (Film-Sense). Electrical conductivity of the films was calculated and compared for the both the as-deposited and water-rinsed films. The transmission spectra were measured using a UV−Vis spectrophotometer (Hitachi U-2000 Spectrophotometer) using bare soda-lime glass as the reference.

AUTHOR INFORMATION

Corresponding Author

Mikko Ritala − *Department of Chemistry, University of Helsinki, Helsinki FI-00014, Finland;* orcid.org/0000-0002-6210-2980; Email: mikko.ritala@helsinki.fi

Authors

Saba Ghafourisaleh − *Department of Chemistry, University of Helsinki, Helsinki FI-00014, Finland;* orcid.org/0000-0003-2944-6973

Georgi Popov − *Department of Chemistry, University of Helsinki, Helsinki FI-00014, Finland;* orcid.org/0000-0003-1233-8327

Markku Leskelä − *Department of Chemistry, University of Helsinki, Helsinki FI-00014, Finland;* orcid.org/0000-0001-5830-2800

Matti Putkonen − *Department of Chemistry, University of Helsinki, Helsinki FI-00014, Finland*

Complete contact information is available at: https://pubs.acs.org/10.1021/acsomega.1c02029

Notes

The authors declare no competing financial interest.

ACKNOWLEDGMENTS

This project has received funding from the European Union's Horizon 2020 research and innovation program under the Marie Skłodowska-Curie grant agreement no. 765378. MP acknowledges funding from the Academy of Finland by the profiling action on Matter and Materials, grant no. 318913.

REFERENCES

(1) Kirchmeyer, S.; Reuter, K. Scientific Importance, Properties and Growing Applications of Poly(3,4-Ethylenedioxythiophene). *J. Mater. Chem.* **2005**, *15*, 2077.

(2) Shirakawa, H.; Louis, E. J.; MacDiarmid, A. G.; Chiang, C. K.; Heeger, A. J. Synthesis of Electrically Conducting Organic Polymers: Halogen Derivatives of Polyacetylene, (CH)X. *J. Chem. Soc. Chem. Commun.* **1977**, *16*, 578−580.

(3) Park, Y. W.; Heeger, A. J.; Druy, M. A.; MacDiarmid, A. G. Electrical Transport in Doped Polyacetylene. *J. Chem. Phys.* **1980**, *73*, 946−957.

(4) Rasmussen, S. C. The Path to Conductive Polyacetylene. *Bull. Hist. Chem.* **2014**, *39*, 64−72.

(5) Cho, B.; Park, K. S.; Baek, J.; Oh, H. S.; Koo Lee, Y.-E.; Sung, M. M. Single-Crystal Poly(3,4-Ethylenedioxythiophene) Nanowires with Ultrahigh Conductivity. *Nano Lett.* **2014**, *14*, 3321−3327.

(6) Heydari Gharahcheshmeh, M.; Robinson, M. T.; Gleason, E. F.; Gleason, K. K. Optimizing the Optoelectronic Properties of Face-On Oriented Poly(3,4-Ethylenedioxythiophene) via Water-Assisted Oxidative Chemical Vapor Deposition. *Adv. Funct. Mater.* **2021**, *31*, 2008712.

(7) Gueye, M. N.; Carella, A.; Faure-Vincent, J.; Demadrille, R.; Simonato, J.-P. Progress in Understanding Structure and Transport Properties of PEDOT-Based Materials: A Critical Review. *Prog. Mater. Sci.* **2020**, *108*, 100616.

(8) Elschner, A.;et al. PEDOT: principles and applications of an intrinsically conductive polymer*CRC press*, 2010.

(9) Groenendaal, L.; Jonas, F.; Freitag, D.; Pielartzik, H.; Reynolds, J. R. Poly(3,4-Ethylenedioxythiophene) and Its Derivatives: Past, Present, and Future. *Adv. Mater.* **2000**, *12*, 481−494.

(10) OUYANG, J. Recent Advances of Intrinsically Conductive Polymers. *Acta Physico-Chimica Sin.* **2018**, *34*, 1211−1220.

(11) Rozlosnik, N. New Directions in Medical Biosensors Employing Poly(3,4-Ethylenedioxy Thiophene) Derivative-Based Electrodes. *Anal. Bioanal. Chem.* **2009**, *395*, 637−645.

(12) Chen, H.-W.; Li, C. PEDOT: Fundamentals and Its Nanocomposites for Energy Storage. *Chinese J. Polym. Sci. (English Ed.)* **2020**, *38*, 435−448.

(13) Yue, R.; Xu, J. Poly(3,4-Ethylenedioxythiophene) as Promising Organic Thermoelectric Materials: A Mini-Review. *Synth. Met.* **2012**, *162*, 912−917.

(14) Rahimzadeh, Z.; Naghib, S. M.; Zare, Y.; Rhee, K. Y. An Overview on the Synthesis and Recent Applications of Conducting Poly(3,4-Ethylenedioxythiophene) (PEDOT) in Industry and Biomedicine. *J. Mater. Sci.* **2020**, *55*, 7575−7611.

(15) Ruiz, V.; Colina, A.; Heras, A.; Lopezpalacios, J. Electropolymerization under potentiodynamic and potentiostatic conditionsSpectroelectrochemical study on electrosynthesis of poly[4,4′-

bis(2-methylbutylthio)-2,2′-bithiophene]. *Electrochim. Acta* **2004**, *50*, 59−67.
(16) Schultheiss, A.; Gueye, M.; Carella, A.; Benayad, A.; Pouget, S.; Faure-Vincent, J.; Demadrille, R.; Revaux, A.; Simonato, J.-P. Insight into the Degradation Mechanisms of Highly Conductive Poly(3,4-Ethylenedioxythiophene) Thin Films. *ACS Appl. Polym. Mater.* **2020**, *2*, 2686−2695.
(17) Hong, K. H.; Oh, K. W.; Kang, T. J. Preparation and properties of electrically conducting textiles byin situ polymerization of poly(3,4-ethylenedioxythiophene). *J. Appl. Polym. Sci.* **2005**, *97*, 1326−1332.
(18) Petsagkourakis, I.; Pavlopoulou, E.; Portale, G.; Kuropatwa, B. A.; Dilhaire, S.; Fleury, G.; Hadziioannou, G. Structurally-Driven Enhancement of Thermoelectric Properties within Poly(3,4-Ethylenedioxythiophene) Thin Films. *Sci. Rep.* **2016**, *6*, 1−8.
(19) Gueye, M. N.; Carella, A.; Massonnet, N.; Yvenou, E.; Brenet, S.; Faure-Vincent, J.; Pouget, S.; Rieutord, F.; Okuno, H.; Benayad, A.; Demadrille, R.; Simonato, J.-P. Structure and Dopant Engineering in PEDOT Thin Films: Practical Tools for a Dramatic Conductivity Enhancement. *Chem. Mater.* **2016**, *28*, 3462−3468.
(20) Brooke, R.; Cottis, P.; Talemi, P.; Fabretto, M.; Murphy, P.; Evans, D. Recent Advances in the Synthesis of Conducting Polymers from the Vapour Phase. *Prog. Mater. Sci.* **2017**, *86*, 127−146.
(21) de Leeuw, D. M.; Kraakman, P. A.; Klaassen, D. B. M.; Mutsaers, C. M. J.; Bongaerts, P. F. G. Electroplating of Conductive Polymers for the Metallization of Insulators. *Synth. Met.* **1994**, *66*, 263−273.
(22) Macher, S.; Schott, M.; Sassi, M.; Facchinetti, I.; Ruffo, R.; Patriarca, G.; Beverina, L.; Posset, U.; Giffin, G. A.; Löbmann, P. New Roll-to-Roll Processable PEDOT-Based Polymer with Colorless Bleached State for Flexible Electrochromic Devices. *Adv. Funct. Mater.* **2020**, *30*, 1906254.
(23) Yadav, P.; Naqvi, S.; Patra, A. Poly(3,4-Ethylenedioxyselenophene): Effect of Solvent and Electrolyte on Electrodeposition, Optoelectronic and Electrochromic Properties. *RSC Adv.* **2020**, *10*, 12395−12406.
(24) Popov, A.; Brasiunas, B.; Damaskaite, A.; Plikusiene, I.; Ramanavicius, A.; Ramanaviciene, A. Electrodeposited Gold Nanostructures for the Enhancement of Electrochromic Properties of Pani−Pedot Film Deposited on Transparent Electrode. *Polymers (Basel)* **2020**, *12*, 2778.
(25) Popov, A.; Brasiunas, B.; Mikoliunaite, L.; Bagdziunas, G.; Ramanavicius, A.; Ramanaviciene, A. Comparative Study of Polyaniline (PANI), Poly(3,4-Ethylenedioxythiophene) (PEDOT) and PANI-PEDOT Films Electrochemically Deposited on Transparent Indium Thin Oxide Based Electrodes. *Polymer (Guildf)* **2019**, *172*, 133−141.
(26) Li, B.; Skorenko, K. H.; Qiu, H.; Mativetsky, J. M.; Dwyer, D. B.; Bernier, W. E.; Jones, W. E. Effects of Interfacial Modification for Vapor Phase Polymerized PEDOT on Glass Substrate. *Synth. Met.* **2020**, *260*, 116293.
(27) Jia, Y.; Shen, L.; Liu, J.; Zhou, W.; Du, Y.; Xu, J.; Liu, C.; Zhang, G.; Zhang, Z.; Jiang, F. An Efficient PEDOT-Coated Textile for Wearable Thermoelectric Generators and Strain Sensors. *J. Mater. Chem. C* **2019**, *7*, 3496−3502.
(28) Shen, L.; Liu, P.; Liu, C.; Jiang, Q.; Xu, J.; Duan, X.; Du, Y.; Jiang, F. Advances in Efficient Polymerization of Solid-State Trithiophenes for Organic Thermoelectric Thin-Film. *ACS Appl. Polym. Mater.* **2020**, *2*, 376−384.
(29) Bilger, D.; Homayounfar, S. Z.; Andrew, T. L. A Critical Review of Reactive Vapor Deposition for Conjugated Polymer Synthesis. *J. Mater. Chem. C* **2019**, *7*, 7159−7174.
(30) Bengasi, G.; Baba, K.; Back, O.; Frache, G.; Heinze, K.; Boscher, N. D. Reactivity of Nickel(II) Porphyrins in oCVD Processes-Polymerisation, Intramolecular Cyclisation and Chlorination. *Chem.—A Eur. J.* **2019**, *25*, 8313−8320.
(31) Bengasi, G.; Desport, J. S.; Baba, K.; Cosas Fernandes, J. P.; De Castro, O.; Heinze, K.; Boscher, N. D.; Heinze, K. Molecular Flattening Effect to Enhance the Conductivity of Fused Porphyrin Tape Thin Films. *RSC Adv.* **2020**, *10*, 7048−7057.
(32) Mirabedin, M.; Vergnes, H.; Caussé, N.; Vahlas, C.; Caussat, B. An out of the Box Vision over Oxidative Chemical Vapor Deposition of PEDOT Involving Sublimed Iron Trichloride. *Synth. Met.* **2020**, *266*, 116419.
(33) Tavakoli, M. M.; Gharahcheshmeh, M. H.; Moody, N.; Bawendi, M. G.; Gleason, K. K.; Kong, J. Efficient, Flexible, and Ultra-Lightweight Inverted PbS Quantum Dots Solar Cells on All-CVD-Growth of Parylene/Graphene/OCVD PEDOT Substrate with High Power-per-Weight. *Adv. Mater. Interfaces* **2020**, *7*, 2000498.
(34) Li, X.; Rafie, A.; Smolin, Y. Y.; Simotwo, S.; Kalra, V.; Lau, K. K. S. Engineering Conformal Nanoporous Polyaniline via Oxidative Chemical Vapor Deposition and Its Potential Application in Supercapacitors. *Chem. Eng. Sci.* **2019**, *194*, 156−164.
(35) Bhattacharyya, D.; Howden, R. M.; Borrelli, D. C.; Gleason, K. K. Vapor Phase Oxidative Synthesis of Conjugated Polymers and Applications. *J. Polym. Sci. Part B Polym. Phys.* **2012**, *50*, 1329−1351.
(36) Chelawat, H.; Vaddiraju, S.; Gleason, K. Conformal, Conducting Poly(3,4-Ethylenedioxythiophene) Thin Films Deposited Using Bromine as the Oxidant in a Completely Dry Oxidative Chemical Vapor Deposition Process. *Chem. Mater.* **2010**, *22*, 2864−2868.
(37) Atanasov, S. E.; Losego, M. D.; Gong, B.; Sachet, E.; Maria, J.-P.; Williams, P. S.; Parsons, G. N. Highly Conductive and Conformal Poly(3,4-Ethylenedioxythiophene) (PEDOT) Thin Films via Oxidative Molecular Layer Deposition. *Chem. Mater.* **2014**, *26*, 3471−3478.
(38) Kaviani, S.; Mohammadi Ghaleni, M.; Tavakoli, E.; Nejati, S. Electroactive and Conformal Coatings of Oxidative Chemical Vapor Deposition Polymers for Oxygen Electroreduction. *ACS Appl. Polym. Mater.* **2019**, *1*, 552−560.
(39) Heydari Gharahcheshmeh, M.; Tavakoli, M. M.; Gleason, E. F.; Robinson, M. T.; Kong, J.; Gleason, K. K. Tuning, Optimization, and Perovskite Solar Cell Device Integration of Ultrathin Poly(3,4-Ethylene Dioxythiophene) Films via a Single-Step All-Dry Process. *Sci. Adv.* **2019**, *5*, No. eaay0414.
(40) Ashurbekova, K.; Ashurbekova, K.; Botta, G.; Yurkevich, O.; Knez, M.; Knez, M. Vapor Phase Processing: A Novel Approach for Fabricating Functional Hybrid Materials. *Nanotechnology* **2020**, *31*, 342001.
(41) Meng, X. An Overview of Molecular Layer Deposition for Organic and Organic-Inorganic Hybrid Materials: Mechanisms, Growth Characteristics, and Promising Applications. *J. Mater. Chem. A* **2017**, *5*, 18326−18378.
(42) Gregorczyk, K.; Knez, M. Hybrid Nanomaterials through Molecular and Atomic Layer Deposition: Top down, Bottom up, and in-between Approaches to New Materials. *Prog. Mater. Sci.* **2016**, *75*, 1−37.
(43) Zhang, Z.; Zhao, Y.; Zhao, Z.; Huang, G.; Mei, Y. Atomic Layer Deposition-Derived Nanomaterials: Oxides, Transition Metal Dichalcogenides, and Metal-Organic Frameworks. *Chem. Mater.* **2020**, *32*, 9056−9077.
(44) Miikkulainen, V.; Leskelä, M.; Ritala, M.; Puurunen, R. L. Crystallinity of Inorganic Films Grown by Atomic Layer Deposition: Overview and General Trends. *J. Appl. Phys.* **2013**, *113* (2), 021301/1−021301/101.
(45) Knox, K.; Coffey, C. E.; Knox, K. Chemistry of Rhenium and Technetium. II. Magnetic Susceptibilities of ReCl5, ReCl3,, TCCL4, and MOCL5,. *J. Am. Chem. Soc.* **1959**, *81*, 5−7.
(46) Heydari Gharahcheshmeh, M.; Gleason, K. K. Texture and Nanostructural Engineering of Conjugated Conducting and Semiconducting Polymers. *Mater. Today Adv.* **2020**, *8*, 100086.
(47) Ha, Y.-H.; Nikolov, N.; Pollack, S. K.; Mastrangelo, J.; Martin, B. D.; Shashidhar, R. Towards a Transparent, Highly Conductive Poly(3,4-Ethylenedioxythiophene). *Adv. Funct. Mater.* **2004**, *14*, 615−622.
(48) Baxamusa, S. H.; Im, S. G.; Gleason, K. K. Initiated and Oxidative Chemical Vapor Deposition: A Scalable Method for Conformal and Functional Polymer Films on Real Substrates. *Phys. Chem. Chem. Phys.* **2009**, *11*, 5227−5240.
(49) McCarthy, J. E.; Hanley, C. A.; Brennan, L. J.; Lambertini, V. G.; Gun'ko, Y. K. Fabrication of Highly Transparent and Conducting

https://doi.org/10.1021/acsomega.1c02029
ACS Omega 2021, 6, 17545−17554

PEDOT:PSS Films Using a Formic Acid Treatment. *J. Mater. Chem. C* **2014**, *2*, 764−770.
(50) Wang, X.; Zhang, X.; Sun, L.; Lee, D.; Lee, S.; Wang, M.; Zhao, J.; Shao-Horn, Y.; Dincă, M.; Palacios, T.; Gleason, K. K. High Electrical Conductivity and Carrier Mobility in OCVD PEDOT Thin Films by Engineered Crystallization and Acid Treatment. *Sci. Adv.* **2018**, *4*, No. eaat5780.
(51) Lee, T.; Kwon, W.; Park, M. Highly Conductive, Transparent and Metal-Free Electrodes with a PEDOT:PSS/SWNT Bilayer for High-Performance Organic Thin Film Transistors. *Org. Electron.* **2019**, *67*, 26−33.
(52) Kee, S.; Kim, N.; Kim, B. S.; Park, S.; Jang, Y. H.; Lee, S. H.; Kim, J.; Kim, J.; Kwon, S.; Lee, K. Controlling Molecular Ordering in Aqueous Conducting Polymers Using Ionic Liquids. *Adv. Mater.* **2016**, *28*, 8625−8631.
(53) Song, J.; Ma, G.; Qin, F.; Hu, L.; Luo, B.; Liu, T.; Yin, X.; Su, Z.; Zeng, Z.; Jiang, Y.; Wang, G.; Li, Z. High-Conductivity, Flexible and Transparent PEDOT: PSS Electrodes for High Performance Semi-Transparent Supercapacitors. *Polymers (Basel)* **2020**, *12*, 450.
(54) Alemu, D.; Wei, H.-Y.; Ho, K.-C.; Chu, C.-W. Highly Conductive PEDOT:PSS Electrode by Simple Film Treatment with Methanol for ITO-Free Polymer Solar Cells. *Energy Environ. Sci.* **2012**, *5*, 9662−9671.
(55) Xia, Y.; Sun, K.; Ouyang, J. Solution-Processed Metallic Conducting Polymer Films as Transparent Electrode of Optoelectronic Devices. *Adv. Mater.* **2012**, *24*, 2436−2440.
(56) Nardes, A. M.; Kemerink, M.; de Kok, M. M.; Vinken, E.; Maturova, K.; Janssen, R. A. J. J. Conductivity, Work Function, and Environmental Stability of PEDOT:PSS Thin Films Treated with Sorbitol. *Org. Electron.* **2008**, *9*, 727−734.
(57) Vosgueritchian, M.; Lipomi, D. J.; Bao, Z. Highly Conductive and Transparent PEDOT:PSS Films with a Fluorosurfactant for Stretchable and Flexible Transparent Electrodes. *Adv. Funct. Mater.* **2012**, *22*, 421−428.
(58) Aasmundtveit, K. E.; Samuelsen, E. J.; Pettersson, L. A. A.; Inganäs, O.; Johansson, T.; Feidenhans'l, R. Structure of Thin Films of Poly(3,4-Ethylenedioxythiophene). *Synth. Met.* **1999**, *101*, 561−564.
(59) Dyuzheva, T. I.; Bendeliani, N. A.; Glushko, A. N.; Kabalkina, S. S. Phase Diagram of ReO_3 up to 10 GPa. *Phys. Scr.* **1989**, *39*, 341−342.
(60) Marciniak, S.; Crispin, X.; Uvdal, K.; Trzcinski, M.; Birgerson, J.; Groenendaal, L.; Louwet, F.; Salaneck, W. R. Light Induced Damage in Poly(3,4-Ethylenedioxythiophene) and Its Derivatives Studied by Photoelectron Spectroscopy. *Synth. Met.* **2004**, *141*, 67−73.
(61) Jönsson, S. K. M.; Birgerson, J.; Crispin, X.; Greczynski, G.; Osikowicz, W.; Denier van der Gon, A. W.; Salaneck, W. R.; Fahlman, M. The Effects of Solvents on the Morphology and Sheet Resistance in Poly(3,4-Ethylenedioxythiophene)-Polystyrenesulfonic Acid (PEDOT-PSS) Films. *Synth. Met.* **2003**, *139*, 1−10.
(62) Greiner, M. T.; Rocha, T. C. R.; Johnson, B.; Klyushin, A.; Knop-Gericke, A.; Schlögl, R. The Oxidation of Rhenium and Identification of Rhenium Oxides during Catalytic Partial Oxidation of Ethylene: An in-Situ Xps Study. *Zeitschrift fur Phys. Chemie* **2014**, *228*, 521−541.
(63) Aubert, P.-H.; Knipper, M.; Groenendaal, L.; Lutsen, L.; Manca, J.; Vanderzande, D. Copolymers of 3,4-Ethylenedioxythiophene and of Pyridine Alternated with Fluorene or Phenylene Units: Synthesis, Optical Properties, and Devices. *Macromolecules* **2004**, *37*, 4087−4098.
(64) Lai, M. K.; Wu, J. R.; Yeh, J. M.; Chang, S. H. Unraveling the Modified PEDOT:PSS Thin Films Based Near-Infrared Solar-Heat Shields by Using Broadband Transmittance and Raman Scattering Spectrometers. *Phys. Status Solidi Appl. Mater. Sci.* **2019**, *216*, 1900025.
(65) Garreau, S.; Louarn, G.; Buisson, J. P.; Froyer, G.; Lefrant, S. In Situ Spectroelectrochemical Raman Studies of Poly(3,4-Ethylenedioxythiophene) (PEDT). *Macromolecules* **1999**, *32*, 6807−6812.
(66) Li, Q.; Yang, J.; Chen, S.; Zou, J.; Xie, W.; Zeng, X. Highly Conductive PEDOT:PSS Transparent Hole Transporting Layer with Solvent Treatment for High Performance Silicon/Organic Hybrid Solar Cells. *Nanoscale Res. Lett.* **2017**, *12*, 506.
(67) Santamaría-Pérez, D.; McGuire, C.; Makhluf, A.; Kavner, A.; Chuliá-Jordán, R.; Pellicer-Porres, J.; Martinez-García, D.; Doran, A.; Kunz, M.; Rodríguez-Hernández, P.; Muñoz, A. Exploring the Chemical Reactivity between Carbon Dioxide and Three Transition Metals (Au, Pt, and Re) at High-Pressure, High-Temperature Conditions. *Inorg. Chem.* **2016**, *55*, 10793−10799.
(68) Purans, J.; Kuzmin, A.; Cazzanelli, E.; Mariotto, G. Disorder-Induced Raman Scattering in Rhenium Trioxide (ReO_3). *J. Phys. Condens. Matter* **2007**, *19*, 226206.

https://doi.org/10.1021/acsomega.1c02029
ACS Omega 2021, 6, 17545−17554